



Indigo-Based Acceptor Type Small Molecules: Synthesis, Electrochemical and Optoelectronic Characterizations

Gözde Murat Saltan¹ · Deniz Aykut Kıymaz² · Ceylan Zafer² · Haluk Dinçalp¹

Received: 12 May 2018 / Accepted: 20 August 2018
© Springer Science+Business Media, LLC, part of Springer Nature 2018

Abstract

In this paper, we report design and synthesis of novel low bandgap small molecules, indigo-benzimidazole (**Tyr-3**) and indigo-schiff base (**Tyr-4**) type acceptors. In these structures, *tert*-butoxycarbonyl (*t*-BOC) group has been attached to indigo nitrogen atom in order to increase the solubility. UV-vis absorption spectra of **Tyr-3** and **Tyr-4** dyes exhibit wide absorption bands ranging from 350 to 600 nm, indicating the relatively low bandgap giving around 2.07 eV for each. Excitation of both **Tyr-3** and **Tyr-4** dyes at 485 nm displays characteristic emission features of indigo moiety and also intramolecular charge transfer complex (ICT) related with their subunits. Besides increasing fluorescence quantum yields as compared to model compound, biexponential decay times for fluorescence life times were also obtained for **Tyr-3** and **Tyr-4** dyes. Their appropriate energy levels along with low HOMO levels are desired for light harvesting acceptors for organic solar cells when blended with poly[N-9'-heptadecanyl-2,7-carbazole-alt-5,5-(4,7-di-2-thienyl-2',1',3'-benzothiadiazole)] (PCDTBT) as donor polymer. Photovoltaic behavior of the synthesized dyes were examined in bulk heterojunction concept and achieved photovoltaic conversion efficiencies were discussed.

Keywords Indigo · Benzimidazole · Fluorescent · Intramolecular charge transfer complex · Bulk heterojunction solar cell

Introduction

Indigo, considerably known for thousands of years, is crucial and popular pigment which has been widely used in textile industries [1, 2]. Natural indigo precursor is extracted from the plants *Indigofera tinctoria* and *Isatis tinctoria* which involve a glucoside called indicant, giving unstable indoxyl molecule in the presence of special enzymes, then oxidized into stable indigo pigment in the presence of atmospheric oxygen [3]. *Tyrian purple*, the 6,6'-dibromo derivative of indigo compound, is well-known in valuable pigment production. It

is produced by extraction of the secretions of a gland for gastropod mollusks living in the Mediterranean basin since ancient times [4]. Indigo has an extraordinarily low solubility in common organic solvents and a high melting point (~390–392 °C), arising from stabilization with strong inter- and intramolecular hydrogen bonding. Their usages are restricted in synthetic organic chemistry because of their low solubilities [3, 5]. As a technique to make indigos processable for chemical synthesis, Glowacki et al. reported that thermolabile *t*-BOC protecting group is attached to indigo nitrogen. Finally, indigo pigment can be suitable for chemical manipulation and processing [3, 6]. However, N,N'-disubstitution with alkyl or acyl units eliminates H-bonding and causes a large deviation from coplanarity of indigo ring, causing blue shift in absorption wavelength of indigo [6, 7].

Indigo and its derivatives are used in many applications for optoelectronic technologies such as organic field-effect transistors (OFETs) [6, 8, 9], organic photodiodes [10], and bulk heterojunction solar cells (BHJ-SCs) [11–13]. Indigo and tyrian purple are intrinsically ambipolar organic semiconductors with electrochemical bandgap values of 1.7 [9, 14] and 1.8 eV [15], respectively, possessing high and well-balanced electron and hole mobilities $\mu_e/\mu_h = 1.0 \times 10^{-2}/0.5-1.0 \times 10^{-2}$ [14] and

Electronic supplementary material The online version of this article (<https://doi.org/10.1007/s10895-018-2287-3>) contains supplementary material, which is available to authorized users.

✉ Haluk Dinçalp
haluk.dincalp@cbu.edu.tr

¹ Department of Chemistry, Faculty of Arts and Science, Manisa Celal Bayar University, Yunus Emre, 45140 Manisa, Turkey

² Solar Energy Institute, Ege University, Bornova, 35100 Izmir, Turkey

$\mu_e/\mu_h = 3.0 \times 10^{-2}/22 \times 10^{-2} \text{ cm}^2/\text{V}\cdot\text{s}$ [15], respectively. Guo et al. reported that a new n-type semiconducting indigo polymer with thermocleavable *t*-BOC group gave electron mobility around $6.0 \times 10^{-3} \text{ cm}^2/\text{V}\cdot\text{s}$ in OFET device after thermal treatment at 170 °C to remove the *t*-BOC groups [7]. Among the limited number of photovoltaic studies for indigo dyes, Lu et al. reported that indigo-doped poly(3-hexylthiophene-2,5-diyl) (P3HT):[6, 6]-phenyl C₆₁-butyric acid methyl ester (PCBM) device gave cell efficiency of 2.55 whereas the device without indigo pigment gave only cell efficiency of 2.14 [12]. Liu et al. fabricated a BHJ-SC device with an inverted structure wherein the photoactive layer of benzodithiophene-indigo type polymer with *t*-BOC group and [6, 6]-phenyl C₇₁-butyric acid methyl ester (PC₇₁BM) at 1:4 weight ratio and reported the cell efficiency of 0.75 for this device without annealing process [13].

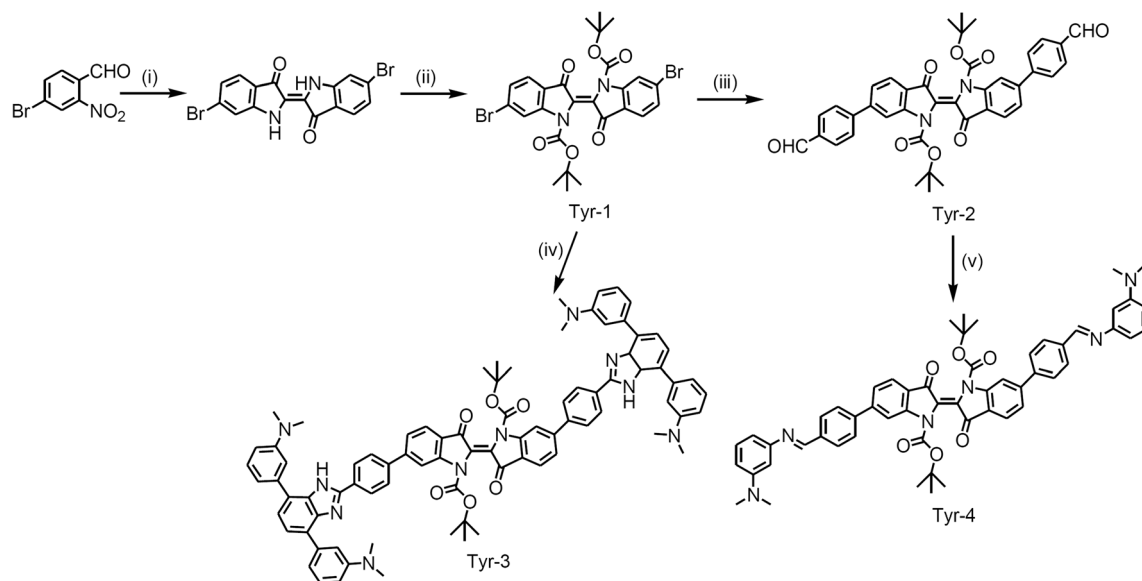
Herein, we have synthesized novel two *t*-BOC functionalized indigo dyes which contain benzimidazole unit for **Tyr-3** and Schiff base unit for **Tyr-4** in their 6,6' positions in order to get a closer look at these conjugated indigos electronic nature in charge transfer processes in addition to optoelectronic performance, specifically in photovoltaics. Benzimidazole and its derivatives constitute an important family of dyes due to their large Stokes shift values and also high fluorescence quantum yields [16]. Optoelectronic properties of the benzimidazoles can be easily tuned by introducing diverse functional groups [17, 18]. In this study, we have investigated electronic contribution of benzimidazole on the optoelectronic performance of indigo dye. We have compared photophysical properties of **Tyr-3** and **Tyr-4** dyes with model compound **Tyr-1** in different

solvents (Scheme 1). We have also investigated their electron-acceptor behaviors as n-type semiconductor in the active layer of BHJ-SC device with p-type PCDTBT donor low band gap conjugated polymer and examined the effect of benzimidazole and Schiff base group on photovoltaic efficiency.

Experimental

Materials and Reagents

Used as the main reagents, 4-Bromo-2-nitrobenzaldehyde, di-*tert*-butyl dicarbonate, 4-formylphenylboronic acid, 4-dimethylaminopyridine, and *tetrakis*(triphenylphosphine)palladium (0) (Pd(PPh₃)₄) were purchased from Sigma Aldrich. Benzene, bromine, hydrogen bromide solution (47%), sodium borohydride, tetrahydrofuran, methanol, and ethanol were purchased from Merck Company. Sodium carbonate (from Carlo Erba) and CoCl₂·6H₂O, N,N-dimethyl-1,3-phenylene diamine dihydrochloride, N,N-dimethyl phenyl boronic acid, and magnesium sulphate (from Alfa Aesar) were used as received. Other reagents and solvents were purchased commercially as analytical-grade quality and used without further purification. **Tyr-3**-benzimidazole precursors, 4,7-Dibromo-2,1,3-benzothiadiazole, (3-{7-[3-(dimethylamino)phenyl]-2,1,3-benzothiadiazole-4-yl}phenyl)dimethylamine, and bis amine N³,N³,N^{3''},N^{3''}-tetramethyl-1,1':4',1''-terphenyl-2',3,3',3''-tetramine were synthesized according to reference [21]. PEDOT:PSS (CLEVIOS™ P VP AI 4083, Heraeus Deutschland GmbH & Co. KG) was purchased from



Scheme 1 Synthetic route to target **Tyr-1**, **Tyr-3**, and **Tyr-4** dyes. (i) Acetone:water (1:1), 1 M NaOH, room temperature [6, 19]; (ii) di-*tert*-butyl-dicarbonate, 4-dimethylaminopyridine (DMAP), THF, room temperature [6]; (iii) THF, 2 M Na₂CO₃, Pd(PPh₃)₄, 4-formylphenylboronic acid, 65 °C [6, 20]; (iv) (4-{4,7-bis[3-

(dimethylamino)phenyl]-1H-benzimidazole-2-yl}phenyl)boronic acid, benzene, 2 M Na₂CO₃, Pd(PPh₃)₄, 85 °C [6, 20]; (v) N,N-dimethyl-1,3-phenylenediamine dihydrochloride, CHCl₃:pyridine solution, addition at -20 °C, then stirring at room temperature.

Aldrich, PCDTBT was purchased from Luminescence Technology Corp. (Lumtec), Taiwan and used as received without further purification.

Analytical Instruments

FT-IR spectra were recorded on a Perkin Elmer-Spectrum BX spectrophotometer with samples prepared as KBr pellets. ^1H NMR (400 MHz) and ^{13}C NMR (100 MHz) spectra were recorded using a Bruker spectrometer. UV-Vis absorption and fluorescence emission spectra were recorded on a Perkin Elmer Lambda 950 and FLS 920 Edinburg spectrophotometers, respectively. Fluorescence quantum yields of the compounds were determined using perylene-3,4,9,10-tetracarboxylic-bis-N,N'-dodecyl diimide (N-DODEPER) ($\Phi_{\text{F}} = 1.0$ in CHCl_3) [22]. Cyclic voltammetry (CV) measurements on compounds **Tyr-1**, **Tyr-3** and **Tyr-4** dyes in MeCN were measured using 100 mM [TBA][PF₆] as the electrolyte in a CH instruments 660B-Electrochemical Workstation at a scan rate of 100 mV/s. Ferrocene was used as the internal standard and its oxidation potential detected at +0.61 V. A glassy carbon working electrode, a platinum wire auxiliary electrode, and an Ag/Ag⁺ reference electrode (SCE) were used in a standard three-electrode configuration cell. The HOMO and LUMO energy levels were calculated according to the following equations [23]:

$$E_{\text{HOMO}} = -e(E_{\text{ox}}^{\text{onset}} + 4.8) \quad ; \quad E_{\text{LUMO}} = -e(E_{\text{red}}^{\text{onset}} + 4.8)$$

$$E_{\text{g}}^{\text{opt}} = 1240 / \lambda_{\text{abs}}^{\text{onset}} ; E_{\text{HOMO}} = E_{\text{LUMO}} - E_{\text{g}}^{\text{opt}}$$

The fluorescence decays of the compounds were obtained with nanosecond resolution at excitation wavelength of 472.4 nm on an apparatus described elsewhere [21] and were analyzed using a nonlinear, exponential tail fit method [24]. The goodness-of-fit was judged from the reduced χ^2 (≤ 1.2) [25]. Non-contact mode atomic force microscopy (AFM) was performed with an Ambios Technology Q-Scope 250 Model instrument.

The minimum energy of geometry was performed in the framework of density functional theory (DFT) [26] by means of the B3LYP using the Gaussian 09 W program. HOMO and LUMO orbitals of the dyes were illustrated by the 6-31G(d) level [27] for stable structures.

Fabrication and Characterization of OPV Devices

BHJ-SCs were fabricated in a regular BHJ arrangement by sandwiching 1:1 or 1:4 (w/w) for PCDTBT:indigo (mixing at concentrations of 2 wt%) film between a transparent ITO/PEDOT:PSS and Al-Ca electrodes. ITO glass substrates were 2.5×2.5 cm in size and $10 \Omega/\text{sq}$ in conductivity. They were cleaned before the coating using the following sequential steps: rinsing with deionized water; sonication in acetone, and isopropanol for 15 min each; and

drying with nitrogen. Then, the substrates were etched with oxygen plasma for 5 min. PEDOT:PSS (AL4083) suspension was filtered and, then spun cast at 4000 rpm for 30 s, followed by annealing at 120 °C for 30 min. **Tyr-1**, **Tyr-3** and **Tyr-4** dyes were dissolved in *o*-dichlorobenzene (20 mg/mL). The photoactive layers containing blends of PCDTBT and indigo dye were coated at 1500 rpm for 1 min and, then annealed at 120 °C for 15 min in an inert-atmosphere glovebox. As a result, thickness of the obtained active layers were measured as 80 nm. Finally, Ca (30 nm)/Al (70 nm) cathode layer was deposited by thermal evaporation with shadow mask giving an active area of 0.16 cm² in thermal evaporator integrated to inert atmosphere glove box. Photovoltaic evaluation of fabricated devices were performed under standard conditions (100 mW.cm⁻² light intensity and AM1.5G irradiation) in inert atmosphere with solar simulator integrated glove box. Current density-Voltage (J-V) measurement were done by using Keithley 2400 source-measure unit and LabView® data acquisition software.

Space-charge-limited current (SCLC) measurements were applied to measure electron mobility of **Tyr-1** in device configuration of FTO/TiO₂(40 nm)/**Tyr-1**(60 nm)/LiF(0.6 nm)/Al(70 nm). **Tyr-1** mobility was determined by fitting the dark current using an equation given below:

$$J_{\text{SCLC}} = \frac{9}{8} \varepsilon_0 \varepsilon_r \mu_e \frac{V^2}{L^3}$$

where ε_0 is the permittivity of free space, ε_r is the dielectric constant of **Tyr-1** film, μ_e is the electron mobility, V is the applied voltage, and L is the thickness of the photo-active layer [28, 29].

Synthesis Procedures

Synthesis of Tyrian Purple

Solution of 1 M NaOH (5 mL) was added to a mixture of 4-Bromo-2-nitrobenzaldehyde in 20 mL of acetone:water (v:v, 1:1) volume percent. The mixture was stirred overnight. The resulting precipitate was collected by suction filtration and, then washed with acetone and distilled water, respectively, yielding 42%. FT-IR (KBr pellet, cm⁻¹): 3640, 3386 (amine $\nu_{\text{N-H}}$), 2955 (aromatic $\nu_{\text{C-H}}$), 1706 (ketone $\nu_{\text{C=O}}$), 1634, 1614, 1578, 1532, 1439, 1387, 1313, 1231, 1158, 1047, 898, 767 cm⁻¹.

Synthesis of Di-tert-butyl (2E)

-6,6'-dibromo-3,3'-dioxo-2,2'-biindole-1,1'(3H,3'H)-dicarboxylate (**Tyr-1**)

A mixture of di-tert-butyl dicarbonate (0.12 g, 604 μmol) and 4-dimethylaminopyridine (DMAP) (24 mg, 196 μmol) in

5 mL of THF were stirred for 15 min at room temperature and, then tyrian purple (30 mg, 71 μmol) was added to the reaction mixture. The mixture was stirred at room temperature for an hour. After completion, the solvent was evaporated and the crude product was purified by column chromatography on silica gel using *n*-hexane:ethyl acetate 4:1 (v:v) as an eluent, yielding 98%. FT-IR (KBr pellet, cm^{-1}): 2963, 2921, 2854 (aliphatic $\nu_{\text{C-H}}$), 1742 (ester $\nu_{\text{C=O}}$), 1677 (ketone $\nu_{\text{C=O}}$), 1597, 1422, 1367, 1273, 1185, 1142, 1085, 1054, 1004, 872, 843 cm^{-1} . ^1H NMR (400 MHz, CDCl_3 δ 7.27 ppm) δ 8.27 (s, 2H), 7.63 (d, $J = 8.1$ Hz, 2H), 7.38 (d, $J = 8.1$ Hz, 2H), 1.61 (s, 18H) ppm. ^{13}C NMR [100 MHz, CDCl_3 δ 77.41 (3 peaks)] δ 183.3, 150.2, 150.0, 131.8, 128.4, 125.6, 122.3, 120.8, 85.7, 28.2 ppm.

Synthesis of Di-tert-butyl (2E)-6,6'-bis(4-formylphenyl)-3,3'-dioxo-2,2'-biindole-1,1'(3H,3'H)-dicarboxylate (Tyr-2)

To a solution of Tyr-1 (30 mg, 48.4 μmol) in 2 mL of THF was added solution of 1 mL 2 M Na_2CO_3 . Subsequently, tetrakis(triphenylphosphine)palladium (0) ($\text{Pd}(\text{PPh}_3)_4$) which was used as a catalyst, was added to the mixture at 45 $^\circ\text{C}$ under an argon atmosphere and the mixture was stirred at 45 $^\circ\text{C}$ for half an hour. Then, 4-formylphenylboronic acid (16 mg, 0.11 mmol) in 1 mL of THF was added to the solution in portions and the mixture was heated at 65 $^\circ\text{C}$ overnight under an argon atmosphere. Then, the reaction mixture was poured into water and extracted with chloroform (3×50 mL). The organic layer was dried over anhydrous magnesium sulfate and evaporated in vacuum to dryness. The residue was separated by column chromatography on silica gel using *n*-hexane:ethyl acetate 4:1 (v:v), yielding 40%. FT-IR (KBr pellet, cm^{-1}): 3374, 2976, 2926, 2853 (aliphatic $\nu_{\text{C-H}}$), 1738 (ester $\nu_{\text{C=O}}$), 1704 (ketone $\nu_{\text{C=O}}$), 1681 (aldehyde $\nu_{\text{C=O}}$), 1604, 1462, 1436, 1370, 1301, 1188, 1150, 1079, 1005, 836, 759 cm^{-1} . ^1H NMR (400 MHz, CDCl_3 δ 7.26 ppm) δ 10.09 (s, 2H), 8.37 (s, 2H), 8.00 (d, $J = 8.1$ Hz, 4H), 7.86 (d, $J = 7.9$ Hz, 2H), 7.83 (d, $J = 8.1$ Hz, 4H), 7.48 (d, $J = 7.9$ Hz, 2H), 1.62 (s, 18H) ppm. ^{13}C NMR [100 MHz, CDCl_3 δ 77.43 (3 peaks)] δ 192.6, 183.9, 150.7, 150.3, 148.1, 146.7, 136.9, 131.0, 128.8, 125.2, 124.3, 123.1, 116.3, 85.2, 28.3 ppm.

Synthesis of (4-{4,7-bis[3-(dimethylamino)phenyl]-1H-benzimidazole-2-yl}phenyl)boronic acid

$\text{N}^3, \text{N}^3, \text{N}^{3''}, \text{N}^{3''}$ -tetramethyl-1,1':4',1''-terphenyl-2',3,3',3'''-tetramine (50 mg, 0.14 mmol) was dissolved in 2 mL of MeCN and 4-formylphenylboronic acid (30 mg, 0.2 mmol) was added to this solution. The mixture was stirred at room temperature overnight and, then the resulting orange precipitates were collected by filtration, washed with methanol, and dried to give target compound, yielding 80%. FT-IR (KBr pellet, cm^{-1}): 3432 (boronic acid $\nu_{\text{O-H}}$), 2923 (aliphatic

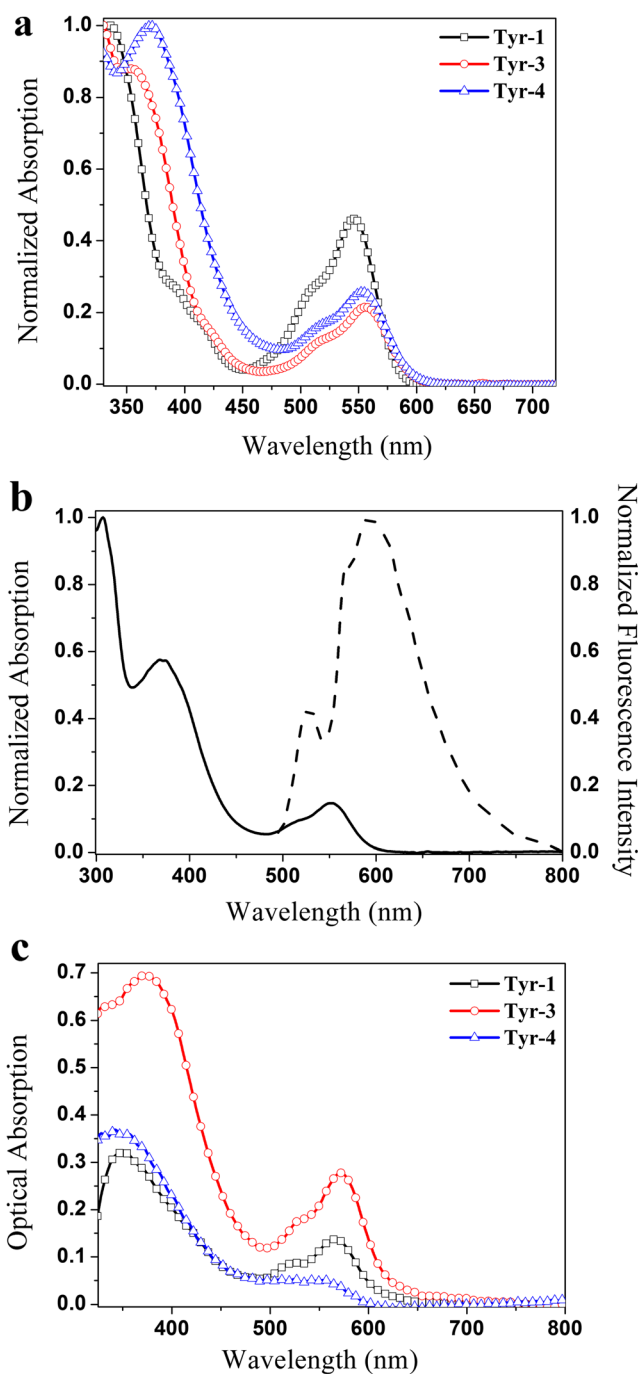


Fig. 1 a Normalized UV-vis absorption spectra of Tyr-1, Tyr-3, and Tyr-4 dyes in toluene solution. b Comparison of normalized UV-vis absorption and fluorescence emission spectra of Tyr-4 in tetrahydrofuran solution ($\lambda_{\text{exc}} = 485$ nm). c UV-vis absorption spectra of Tyr-1, Tyr-3, and Tyr-4 films on ITO-coated glass

$\nu_{\text{C-H}}$), 1609, 1384, 1265, 670 cm^{-1} . ^1H NMR (400 MHz, DMSO-d_6 δ 2.49 ppm) δ 10.04 (s, 1H), 9.79 (s, 1H), 8.29 (d, $J = 8.4$ Hz, 2H), 8.14 (d, $J = 10.6$ Hz, 2H), 7.98 (d, $J = 10.6$ Hz, 1H), 7.92 (d, $J = 8.4$ Hz, 1H), 7.86 (d, $J = 7.9$ Hz, 2H), 7.76 (d, $J = 3.4$ Hz, 2H), 7.34 (s, 2H), 6.93 (d, $J = 10.6$ Hz, 2H), 6.49 (s, 1H), 3.00 (s, 12H) ppm. ^{13}C NMR

Table 1 Long-wavelength absorption (λ (nm)) and emission wavelengths (λ_{em} (nm)) of **Tyr-1**, **Tyr-3**, and **Tyr-4** dyes in different solvents ($\lambda_{exc} = 485$ nm)

Dyes / Solvents	PhCH ₃				CHCl ₃				THF				BzCN			
	λ_1	λ_2	λ_{em1}	λ_{em2}	λ_1	λ_2	λ_{em1}	λ_{em2}	λ_1	λ_2	λ_{em1}	λ_{em2}	λ_1	λ_2	λ_{em1}	λ_{em2}
Tyr-1	545	337	597	-	546	341	605	-	544	335	596	-	547	334	593	531
Tyr-3	557	359	614	582	558	360	606	561	555	357	608	572	559	358	610	576
Tyr-4	553	371	596	536	556	376	582	534	552	371	591	528	556	373	531	511

[100 MHz, CDCl₃ δ 40.22 (7 peaks)] δ 195.0, 192.4, 164.7, 160.3, 153.3, 151.9, 138.4, 135.7, 135.4, 133.2, 129.6, 129.4, 127.4, 116.9, 64.8 ppm.

Synthesis of Di-tert-butyl (2E)

-5,5'-bis(4-{4,7-bis[3-(dimethylamino)phenyl]}

-1H-benzimidazole-2-yl}phenyl)

-3,3'-dioxo-2,2'-biindole-1,1'(3H,3'H)-dicarboxylate (**Tyr-3**)

To a 25 ml two-necked round-bottomed flask were added **Tyr-1** (38 mg, 61.3 μ mol) in 8 mL of benzene and Na₂CO₃ (2 M, 4 mL). A solution of (4-{4,7-bis[3-(dimethylamino)phenyl]-1H-benzimidazole-2-yl}phenyl)boronic acid (65 mg, 0.14 mmol) in 3 mL of ethanol was added to two-necked flask in small portions at 65 °C under an argon atmosphere. Catalytic amount of Pd(PPh₃)₄ was added to the solution and the solution was stirred at 85 °C for 7 h. Small amount of water was poured into the solution. The reaction mixture was extracted with chloroform and concentrated under vacuum. The resulting solid was purified by preparative layer chromatography using *n*-hexane:ethyl acetate 35:15 (v:v) as an eluent, yielding 8%. FT-IR (KBr pellet, cm⁻¹): 2923, 2854 (aliphatic ν_{C-H}), 1732 (ester $\nu_{C=O}$), 1703 (ketone $\nu_{C=O}$), 1674, 1605, 1434, 1367, 1269, 1189, 1149, 1082, 1003, 824 cm⁻¹. ¹H NMR (400 MHz, CDCl₃ δ 7.28 ppm) δ 10.12 (s, 2H), 8.40 (s, 2H), 8.05–8.01 (m, 6H), 7.90–7.81 (m, 8H), 7.51 (d, $J = 9.4$ Hz, 2H), 7.31 (t, $J = 8.3$ Hz, 4H), 6.96 (d, $J = 8.3$ Hz, 8H), 6.75 (dd, $J = 8.3, 2.7$ Hz, 4H), 3.00 (s, 24H), 1.64 (s, 9H), 1.26 (s, 9H) ppm. ¹³C NMR [100 MHz, CDCl₃ δ 77.40 (3 peaks)] δ 192.6, 150.7, 150.4, 146.7, 143.7, 136.9, 136.0, 135.2, 134.7, 134.3, 131.8, 131.0, 130.4, 128.9, 125.2, 124.3, 123.2, 120.2, 116.4, 85.2, 29.8, 28.2, 22.7 ppm.

Synthesis of Di-tert-butyl (2E)-6,6'-bis[4-(E)

-[3-(dimethylamino)phenyl]imino}methyl}phenyl]

-3,3'-dioxo-2,2'-biindole-1,1'(3H,3'H)-dicarboxylate (**Tyr-4**)

A solution of **Tyr-2** (30 mg, 44.7 μ mol) in 0.6 mL of chloroform was cooled to -20 °C. Moreover, N,N-dimethyl-1,3-phenylenediamine dihydrochloride (21 mg, 0.10 mmol) was dissolved in 1 mL of chloroform:pyridine (v:v, 1:1) and this

solution was added slowly into the **Tyr-2** solution. The reaction mixture was stirred at room temperature overnight. After the complementation, the reaction mixture was extracted with purified water, followed by HCl-acidified water. The organic layer was dried over anhydrous magnesium sulfate and

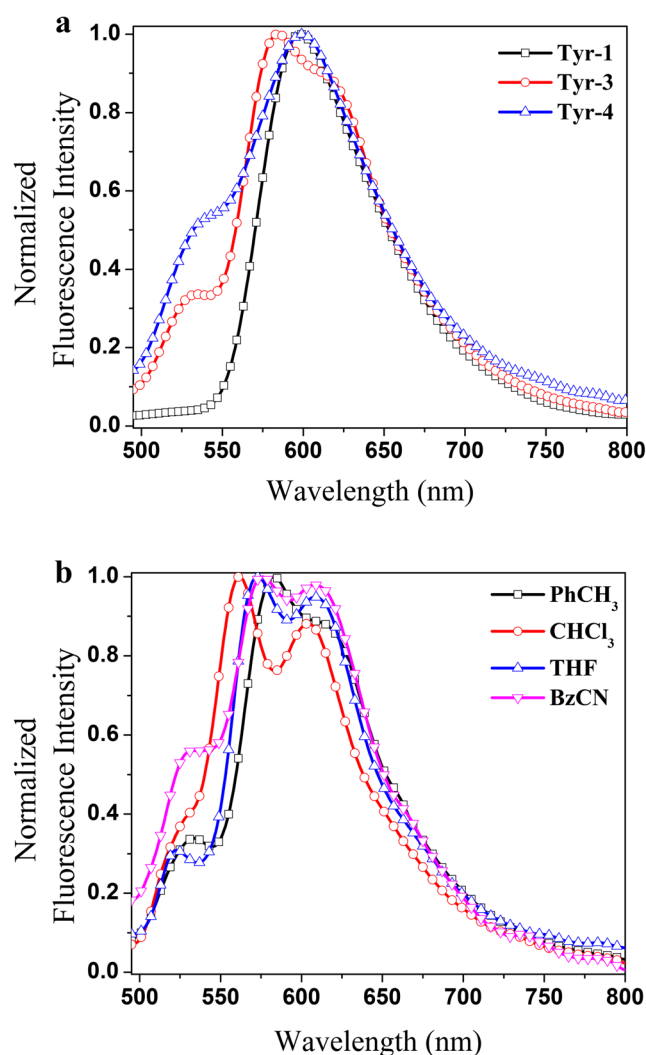
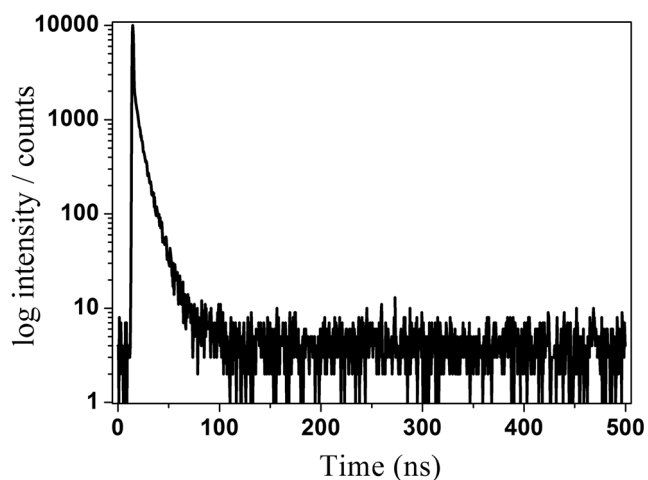


Fig. 2 **a** Normalized fluorescence emission spectra of **Tyr-1**, **Tyr-3**, and **Tyr-4** dyes in toluene solution. **b** Comparison of normalized fluorescence emission spectra of **Tyr-3** in different solvents ($\lambda_{exc} = 485$ nm)

Table 2 Fluorescence quantum yields (Φ_F), fluorescence decay times (τ_F (ns)) with amplitudes, and mean fluorescence lifetimes (τ_m) for **Tyr-1**, **Tyr-3**, and **Tyr-4** dyes in different solvents ($\lambda_{exc} = 485$ nm)

Dyes / Solvents	χ^2	$\tau_{F(1)}$	α_1	$\tau_{F(2)}$	α_2	τ_m	Φ_F	
Tyr-1	Ph-CH ₃	1.08	4.81	-	-	-	0.0137	
	CHCl ₃	0.67	4.45	-	-	-	0.0081	
	THF	0.84	4.16	-	-	-	0.0170	
	Bz-CN	0.76	3.29	38.9	10.05	61.1	7.42	0.0365
Tyr-3	Ph-CH ₃	0.78	3.47	62.6	7.73	37.4	5.06	0.0980
	CHCl ₃	0.87	3.39	69.7	6.68	30.3	4.38	0.0633
	THF	0.86	2.12	22.8	5.67	77.2	4.86	0.1307
	Bz-CN	1.10	2.50	43.9	7.67	56.1	5.40	0.3050
Tyr-4	Ph-CH ₃	0.84	2.98	24.2	10.24	75.8	8.48	0.0147
	CHCl ₃	0.87	3.86	65.8	12.45	34.2	6.79	0.0287
	THF	1.12	4.36	42.2	11.02	57.8	8.20	0.0052
	Bz-CN	0.94	5.54	83.2	10.72	16.8	6.41	0.2274

evaporated in vacuum to dryness. **Tyr-4** was precipitated with chloroform:*n*-hexane binary solvent system, yielding 90%. FT-IR (KBr pellet, cm⁻¹): 3440, 2969, 2923, 2845 (aliphatic ν_{C-H}), 1717 (ester $\nu_{C=O}$), 1681 (ketone $\nu_{C=O}$), 1606 ($\nu_{C=N}$), 1516, 1478, 1435, 1369, 1276, 1150, 1082, 847 cm⁻¹. ¹H NMR (400 MHz, CDCl₃ δ 7.27 ppm) δ 8.34 (s, 2H), 7.83 (d, $J = 8.3$ Hz, 4H), 7.63 (d, $J = 7.1$ Hz, 2H), 7.59–7.36 (m, 6H), 7.32 (d, $J = 8.3$ Hz, 2H), 6.60 (d, $J = 8.3$ Hz, 2H), 6.22–6.03 (m, 6H), 2.91 (s, 12H), 1.64 (s, 18H) ppm. ¹³C NMR [100 MHz, CDCl₃ δ 77.43 (3 peaks)] δ 181.7, 161.8, 131.1, 131.0, 130.9, 130.8, 130.4, 128.2, 122.8, 118.6, 117.3, 114.9, 114.6, 111.9, 107.1, 104.3, 102.6, 101.2, 101.1, 98.3, 40.7, 28.3 ppm.

**Fig. 3** Fluorescence decay graph of **Tyr-4** dye in tetrahydrofuran solution ($\lambda_{detection} = 600$ nm)

Results and Discussion

Optical Properties

The UV—visible absorption spectra of the synthesized indigo dyes in toluene solution are shown in Fig. 1a, and all optical data are summarized in Table 1. Model dye **Tyr-1** gave two major absorption bands, the first absorption band is peaked at 545 nm, and the second band is observed at 337 nm in toluene solution. Indeed, tyrian purple has absorption maximum at 601 nm in DMF solution [30]. Striking blue shift in **Tyr-1** absorption is attributed to the loss of the H-chromophore nature of tyrian purple because of the distorted planarity of indigo ring initiated by N-substitution with *t*-BOC group. **Tyr-3** with benzimidazole donor showed similar optical behavior but its low energy absorption was further red-shifted by 12 nm and, also gave a new absorption band at 359 nm. **Tyr-4** with Schiff base donor showed similar absorption profile giving a red-shifted indigo band with maximum at 553 nm, and a new band at 371 nm. Both renewed bands observed at 359 and 371 nm for **Tyr-3** and **Tyr-4**, respectively, were assigned to the formation of charge transfer state, which will be discussed in the following statements. UV—visible absorption spectra of **Tyr-3** and **Tyr-4** dyes in other studied solvents were given in Fig. S1(a-b).

Issa et al. reported the formation of intramolecular charge transfer complex (ICT) for 3-amino-1,2,4-triazole Schiff bases around 370 nm as a result of the π -delocalized electron cloud of Schiff group [31]. Also, Gan et al. explained the outstanding optical properties of carbazole-Schiff base derivatives by ICT between carbazole donor and acceptor Schiff base [32]. In our measurements, when excited in THF solution at 485 nm (Fig. 1b), **Tyr-4** dye displays characteristic emission band of indigo main core at 591 nm and, also gives a new emission

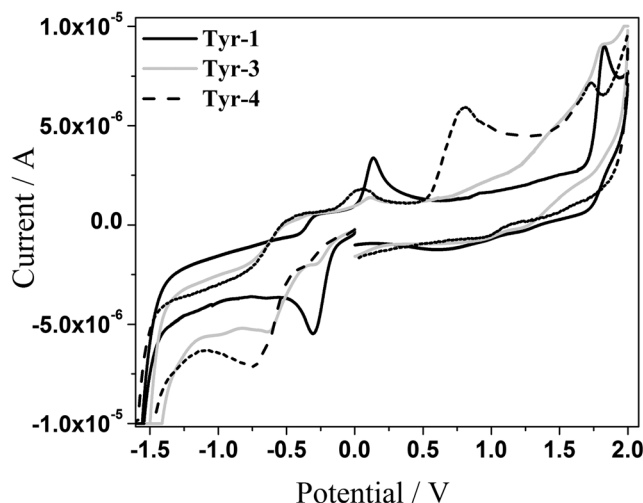
**Fig. 4** Cyclic voltammograms of **Tyr-1**, **Tyr-3**, and **Tyr-4** dyes on glassy carbon working electrode in 0.1 M [TBA][PF₆]/Me-CN (Scan rate: 100 mV s⁻¹)

Table 3 Electrochemical values and HOMO-LUMO energies of **Tyr-1**, **Tyr-3**, and **Tyr-4** dyes with respect to the vacuum level

Dyes	E_{red2}^0 (V)	E_{red1}^0 (V)	E_{ox1}^0 (V)	E_{ox2}^0 (V)	E_{ox3}^0 (V)	LUMO (eV)	HOMO (eV)	E_{0-0}^a (eV)(abs)
Tyr-1	-	-0.29	0.13	1.82	-	-3.90	-6.01	2.11
Tyr-3	-0.62	-0.28	0.11	1.80	-	-3.91	-5.98	2.07
Tyr-4	-0.74	-0.40	0.05	0.79	1.73	-3.79	-5.86	2.07

^a The zeroth-zeroth transition E_{0-0} values were estimated from the intersection of the apsis and the straight line which is drawn from the red side of the UV-vis absorption band in toluene solution

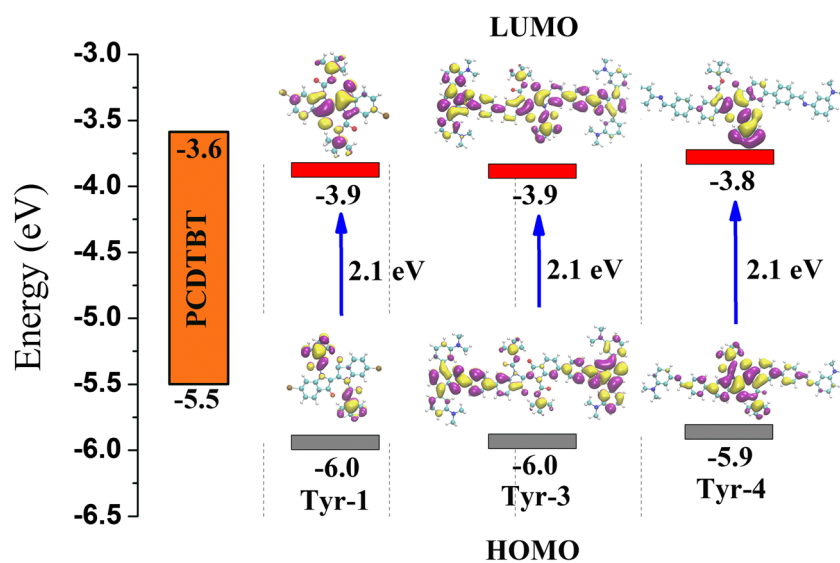
band around at 528 nm, most probably indicating a new specie caused by the Schiff base-related charge transfer complex. Figure 1c depicts the UV-visible absorption spectra of **Tyr-1**, **Tyr-3** and **Tyr-4** in film state, showing similar vision as given in solution phase, but giving red-shifted indigo absorptions with maxima at 567, 573, and 557 nm, respectively.

Figure 2a illustrates the comparison of normalized fluorescence emission spectra of **Tyr-1**, **Tyr-3**, and **Tyr-4** dyes in toluene solution. At the excitation wavelength of 485 nm, while **Tyr-1** brings about only one emission band located at 597 nm, **Tyr-3** dye like **Tyr-4** shows interestingly two emission bands, one of which is observed around 614 nm, and the other one, minor band, is observed at 582 nm. The low energy emission band of **Tyr-3** is more red-shifted as compared to that of **Tyr-1** because of the strongly intermolecular hydrogen bonding between benzimidazole N-H hydrogen and *t*-BOC carbonyl group. More importantly, high energy emission band of **Tyr-3** does not belong to indigo nature. Figure 2b monitors the uncommon emission bands for indigo nature in the structure of **Tyr-3** in different solvents. When **Tyr-3** is excited at 485 nm, in which is mostly indigo but also benzimidazole/indigo ground state complex-related absorption band, the dye displays characteristic emission features of benzimidazole in

high energy and indigo core emission in low energy region. This observation is assigned to ICT complex between the benzimidazole and indigo core. Similar ICT possibilities of benzimidazole for different structures are reported in the literature [21, 33, 34]. Fluorescence emission spectra of **Tyr-3** and **Tyr-4** dyes in other studied solvents were given in Fig. S2(a-b).

Table 2 summarizes fluorescence decay times and fluorescence quantum yields of synthesized indigo series. Also, we have calculated the mean fluorescence lifetimes ($\tau_m = \alpha_1\tau_1 + \alpha_2\tau_2$) for bi-exponential decays. Single photon timing measurement for one of the selected indigo dye, **Tyr-4** dye, in THF solution is shown in Fig. 3. The decays collected in indigo emission at 600 nm were found to fit to a mono-exponential for **Tyr-1** dye around 4 ns in the studied solvents, except Bz-CN solution. **Tyr-1** dye gave an extra emission band at 531 nm in addition to observed bi-exponential decay fit, indicating the formation of ICT complex in more polar Bz-CN solution cages. The lifetimes of **Tyr-3** dye can be analyzed as bi-exponential with short decay times around 2.12–3.47 ns and long decay times around 5.67–7.73 ns. Long decay times with moderately high amplitude values were attributed to the delayed fluorescence caused by the existence of ICT complex

Fig. 5 Electronic structures of the HOMO and LUMO for **Tyr-1**, **Tyr-3**, and **Tyr-4** dyes and comparison of their energy levels with PCDTBT energy alignment



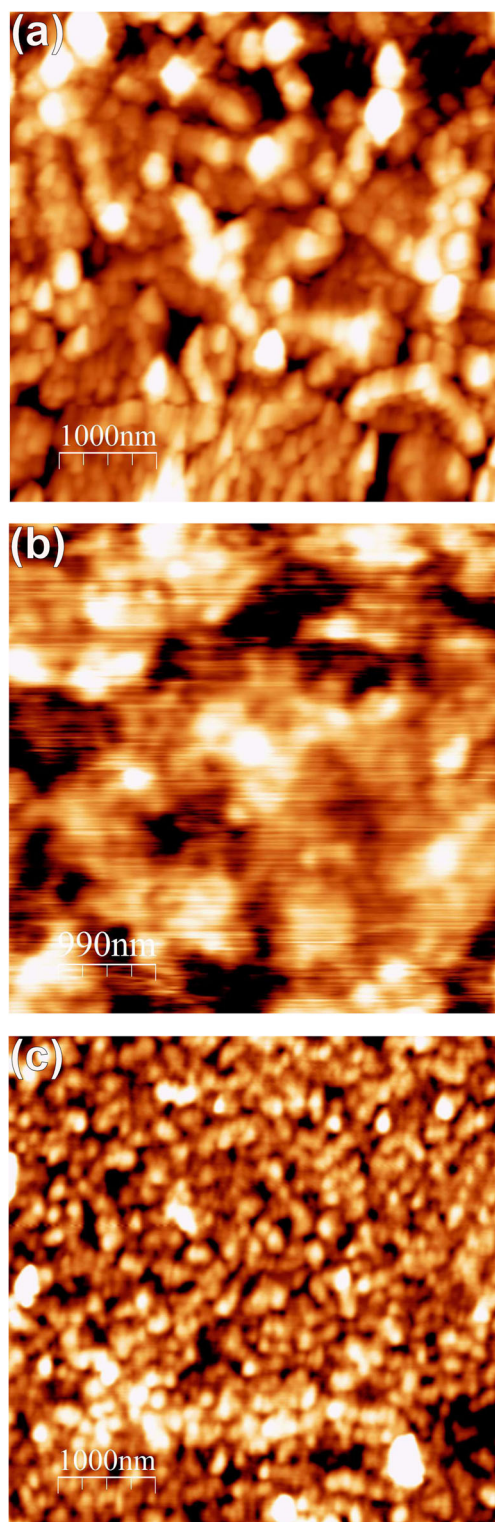


Fig. 6 AFM images ($5 \mu\text{m} \times 5 \mu\text{m}$) of **a** Tyr-1, **b** Tyr-3, and **c** Tyr-4 films spin-coated from chloroform solution

between the benzimidazole donor and indigo acceptor. ICT possibilities of indigo nature was known in the literature for different substituents. Pina et al. reported that charge transfer occurs in indigo-fluorene type copolymers from the fluorene

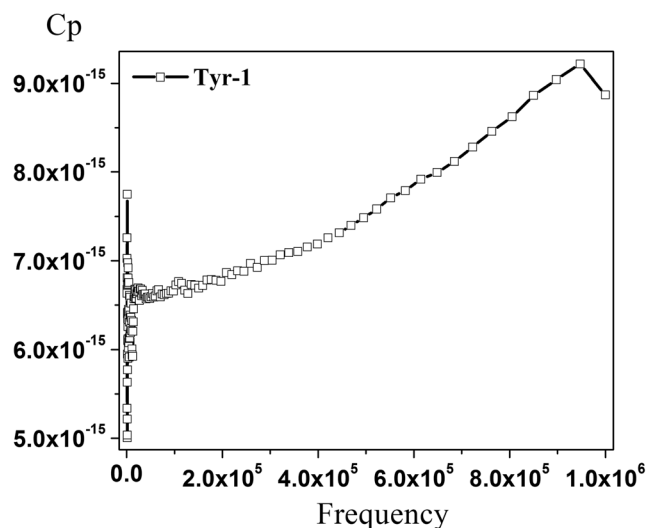


Fig. 7 The variation in the capacitance-frequency (C-F) characteristic of FTO/TiO₂/Tyr-1/LiCl/Al devices

to indigo moiety when the copolymer is excited at fluorine absorption region [35]. Similar results were analyzed for **Tyr-4** dye with Schiff base derivative. **Tyr-4** dye gave bi-exponential decay times, one of which is short decay times around 2.98–5.54 ns, and the long decay times are observed around 10.24–12.45 ns. Short decay times belong to indigo lifetime value, but long decay times are more probably related to existence of complex structure.

Fluorescence quantum yields (Φ_F) of **Tyr-1** dye was calculated to be about between 0.0081–0.0365 in different solvent of polarities. It is reported that Φ_F value of indigo is quite low (Φ_F :0.0023 in DMF) due to its efficient internal conversion radiationless process which may be related to intra- or inter-molecular transfer reactions in H-chromophores of indigo

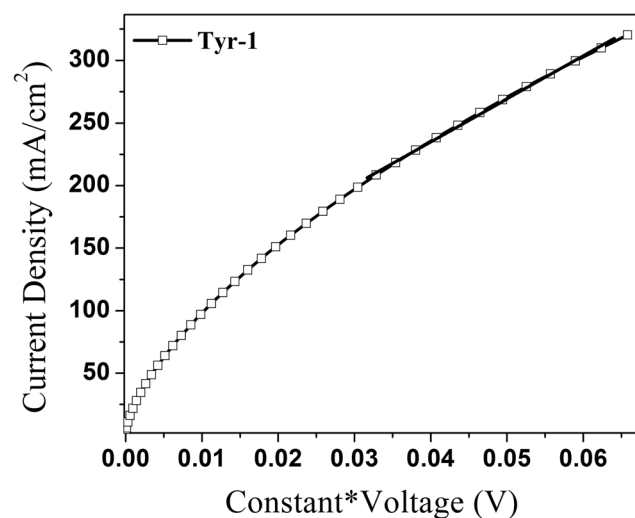


Fig. 8 Dark current density-effective voltage characteristic of SCLC mobility in FTO/TiO₂/Tyr-1/LiCl/Al device

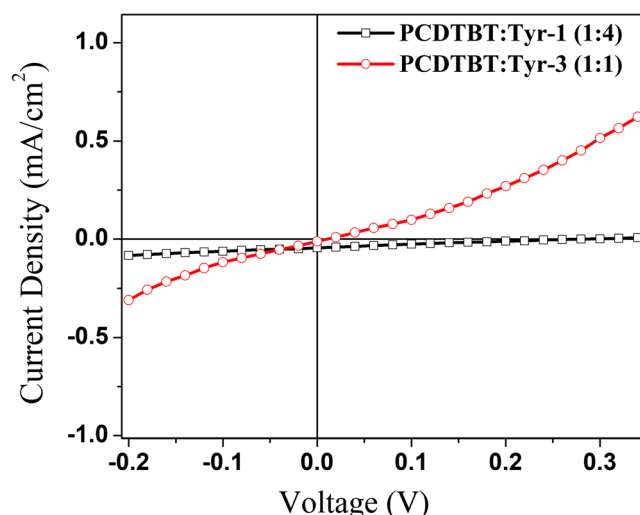


Fig. 9 J-V curves of photovoltaic devices using PCDTBT:Tyr-1, PCDTBT:Tyr-3 blends as active layer

nature [36]. This kind of reactions are inhibited by the N-substitution of indigo with *t*-BOC group in **Tyr-1** structure so that Φ_F value increases. Φ_F values for both **Tyr-3** and **Tyr-4** dyes are quite higher than those presented by **Tyr-1**. Nothing that our synthesized **Tyr-3** and **Tyr-4** dyes gained an extra emission band in high energy region because of the contribution of benzimidazole or Schiff base moieties resulting much higher Φ_F values as compared to that of **Tyr-1** dye. Those higher Φ_F values for **Tyr-3** and **Tyr-4** dyes may also be referred to ICT complex formation. Other striking results are obtained in Bz-CN solution giving somewhat higher Φ_F values as compared to that of other studied solutions. This may be related to existence of ICT complex in more polar Bz-CN solution.

Electrochemical Properties

Figure 4 shows the cyclic voltammetry (CV) diagram of synthesized indigo type small molecules in order to estimate their energy levels. Table 3 summarizes the electrochemical data of the CV measurements. The oxidation potentials of **Tyr-1** are 0.13 and 1.82 V *versus* Ag/Ag⁺. The reduction potential of **Tyr-1** is -0.29 V, indicating the formation of stable indigo anion radical. Both new indigo derivatives present two consecutive reduction peaks at -0.28 and -0.62 V for **Tyr-3**, and

Table 4 OPV parameters of conventional devices prepared from the synthesized indigo dyes as acceptor

Active Layer		V_{oc} (mV)	I_{sc} (mA/cm ²)	FF	η
Binary Structure	w:w				
PCDTBT: Tyr-1	1:4	460	0.10	0.21	0.010
PCDTBT: Tyr-3	1:1	20	0.01	0.86	0.002

at -0.40 and -0.74 V for **Tyr-4** dyes. In the oxidation region, while two oxidation peaks appear at 0.11, and 1.80 V for **Tyr-3**, an extra peak at 0.05 V was observed in addition to 0.79, and 1.73 V for **Tyr-4** dye. This additional peak at 0.05 V is an accordance with the oxidation state of Schiff base group which may be observed independently. The much easier oxidation of **Tyr-3** at 0.11 V is attributed to the presence of benzimidazole group decorated with four electron donor N(CH₃)₂ substituents as compared to the other dyes. The LUMO and HOMO energies of **Tyr-1**, **Tyr-3**, and **Tyr-4**, estimated by CV, are -3.90, -3.91, and -3.79 eV, and -6.01, -5.98, and -5.86 eV, respectively. After introducing the Schiff base unit to the indigo core, **Tyr-4** dye gave a higher LUMO and HOMO level as compared to the other dyes.

Figure 5 compares the energy level of PCDTBT donor polymer with HOMO and LUMO levels of the dye structures which is illustrated by DFT-calculated orbital contours. For **Tyr-1** dye, the HOMO is mainly contributed by the peripheral *t*-BOC groups while the LUMO is delocalized over the mainly indigo region. From the electronic distributions in the molecular orbital contours of **Tyr-3** dye a certain amount of charge may be transferred from the benzimidazole side to the acceptor indigo core. However, while there is little contribution to the HOMO from the peripheral Schiff base groups in **Tyr-4** molecule, LUMO delocalization mainly occurs onto both indigo core and one of the *t*-BOC groups. The LUMO levels of these indigo dyes were well-matched with the LUMO level of donor PCDTBT polymer (-3.6 eV), which is enough level for electron injection and charge separation processes.

Optoelectronic Performance and Morphological Studies

The morphology of thin films spin-coated from chloroform solution of dyes was investigated by AFM images (Fig. 6a-c). The root-mean-square (rms) of surface roughness was 15.4, 8.8 and 2.2 nm for **Tyr-1**, **Tyr-3**, and **Tyr-4**, dyes, respectively. It is noted that only **Tyr-4** layer depicted smooth and uniform film formation.

Electron-only diode were fabricated from thin films of **Tyr-1** dye to understand the electron transport behavior of the material. Capacitance-frequency (C-F) and dark current density-effective voltage characteristics for FTO/TiO₂/**Tyr-1**/LiCl/Al devices were illustrated in Figs. 7 and 8, respectively. SCLC electron mobility of 3.4×10^{-3} cm²/Vs for **Tyr-1** dye was measured. Wherein electron mobilities of other dyes could not be measured because of poor film formation qualities. Obtained electron mobility value for **Tyr-1** is much lower compared to reported values for pristine indigo structure (1×10^{-2} cm²/Vs) [14]. This may be assigned to the formation of more disordered films of **Tyr-1** dye caused by the branched *t*-BOC groups that inhibit the molecular reorganization. Similar indigo derivative in the literature with branched long alkyl

surface group gave the lowest electron mobility value around $5 \times 10^{-2} \text{ cm}^2/\text{Vs}$ because of its unsymmetrical structure in which reduces the intermolecular interactions for neat film formation [10].

BHJ-SCs were fabricated with a conventional structures of ITO/PEDOT:PSS/PCDTBT:dyes/LiCl/Al (70 nm)/Ca (30 nm), wherein the photoactive layer with synthesized indigo series as acceptor. Figure 9 shows the J-V curves of photovoltaic devices using PCDTBT:**Tyr-1**, PCDTBT:**Tyr-3** blends as active layer, and extracted photovoltaic data are summarized in Table 4. The optimal device of **Tyr-1** dye was fabricated by the 20:80 donor:acceptor ratio, giving a short circuit current (I_{sc}) of $0.1 \text{ mA}/\text{cm}^2$, an open circuit voltage (V_{oc}) of 460 mV, a fill factor (FF) of 0.21 and a power conversion efficiency (PCE) of 0.010%. While **Tyr-4** dye did not give any photovoltaic response from the measurements, **Tyr-3** dye showed the much lower device performance obtained with a 50:50 donor:acceptor ratio, giving a I_{sc} of $0.01 \text{ mA}/\text{cm}^2$, a V_{oc} of 20 mV, a FF of 0.86 and a PCE of 0.002% as compared to **Tyr-1** dye.

Conclusions

In summary, we have synthesized a novel class of *t*-BOC functionalized indigo type small molecules which contain benzimidazole or Schiff base unit in 6,6' position in the structure and evaluated the charge transfer possibilities by comparing their optical and electrochemical properties. New generated UV-vis and uncommon emission bands of **Tyr-3** and **Tyr-4** dyes were assigned to the formation of charge transfer state. Interestingly, long decay times for the dye solutions support to the delayed fluorescence caused by the ICT complex between the subunits and acceptor indigo core. We have also utilized them as electron acceptors in molecular BHJ-SC devices for the first time. Although tested indigo dyes did not exhibited superior solar cell efficiencies, indigo derivative dyes will be considered as promising materials for photovoltaic devices if their structures can be improved for better charge transfer abilities.

Acknowledgements This work was supported by the Scientific and Technological Research Council of Turkey (TUBITAK) with the project number of 113Z250. The authors acknowledge the Ege University for theoretical DFT calculations.

References

- Robb MJ, Ku S-Y, Brunetti FG, Hawker CJ (2013) A renaissance of color: New structures and building blocks for organic electronics. *J Polym Sci Pol Chem* 51:1263–1271
- Fukumoto H, Nakajima H, Kojima T, Yamamoto T (2014) Preparation and chemical properties of π -conjugated polymers containing indigo unit in the main chain. *Mater* 7:2030–2043
- Głowacki ED, Voss G, Leonat L, Irimia-Vladu M, Bauer S, Sariciftci NS (2012) Indigo and tyrian purple - from ancient natural dyes to modern organic semiconductors. *Isr J Chem* 52:540–551
- Imming P, Imhof I, Zentgraf M (2006) An improved synthetic procedure for 6,6'-dibromoindigo (tyrian purple). *Synth Commun* 31:3721–3727
- Pitayatanakul O, Iijima K, Kadoya T, Ashizawa M, Kawamoto T, Matsumoto H, Mori T (2015) Ambipolar organic field-effect transistors based on indigo derivatives. *Eng J* 19:61–74
- Głowacki ED, Apaydin DH, Bozkurt Z, Monkowius U, Demirak K, Tordin E, Himmelsbach M, Schwarzinger C, Burian M, Lechner RT, Demitri N, Voss G, Sariciftci NS (2014) Air-stable organic semiconductors based on 6,6'-dithienylindigo and polymers thereof. *J Mater Chem C* 2:8089–8097
- Guo C, Quinn J, Sun B, Li Y (2015) An indigo-based polymer bearing thermocleavable side chains for n-type organic thin film transistors. *J Mater Chem C* 3:5226–5232
- Pitayatanakul O, Higashino T, Kadoya T, Tanaka M, Kojima H, Ashizawa M, Kawamoto T, Matsumoto H, Ishikawa K, Mori T (2014) High performance ambipolar organic field-effect transistors based on indigo derivatives. *J Mater Chem C* 2:9311–9317
- Pitayatanakul O, Iijima K, Ashizawa M, Kawamoto T, Matsumoto H, Mori T (2015) An iodine effect in ambipolar organic field-effect transistors based on indigo derivatives. *J Mater Chem C* 3:8612–8617
- Kim IK, Li X, Ullah M, Shaw PE, Wawrzinek R, Namdas EB, Lo SC (2015) High-performance, fullerene-free organic photodiodes based on a solution-processable indigo. *Adv Mater* 27:6390–6395
- Głowacki ED, Voss G, Demirak K, Havlicek M, Sungner N, Okur AC, Monkowius U, Gasiorowski J, Leonat L, Sariciftci NS (2013) A facile protection-deprotection route for obtaining indigo pigments as thin films and their applications in organic bulk heterojunctions. *Chem Commun (Camb)* 49:6063–6065
- Lu Y-M, Wong J-S, Hsu L-C (2013) Characterization of indigo-doped poly(3-hexylthiophene):[6,6]-phenyl C_{61} -butyric acid methyl ester bulk heterojunction solar cells. *Thin Solid Films* 529:58–61
- Liu C, Dong S, Cai P, Liu P, Liu S, Chen J, Liu F, Ying L, Russell TP, Huang F, Cao Y (2015) Donor-acceptor copolymers based on thermally cleavable indigo, isoindigo, and DPP units: synthesis, field effect transistors, and polymer solar cells. *ACS Appl Mater Interfaces* 7:9038–9051
- Irimia-Vladu M, Glowacki ED, Troshin PA, Schwabegger G, Leonat L, Susarova DK, Krystal O, Ullah M, Kanbur Y, Bodea MA, Razumov VF, Sitter H, Bauer S, Sariciftci NS (2012) Indigo—a natural pigment for high performance ambipolar organic field effect transistors and circuits. *Adv Mater* 24:375–380
- Głowacki ED, Leonat L, Voss G, Bodea M-A, Bozkurt Z, Ramil AM, Irimia-Vladu M, Bauer S, Sariciftci NS (2011) Ambipolar organic field effect transistors and inverters with the natural material tyrian purple. *AIP Adv* 1(1–6):042132
- Çimen O, Dinçalp H, Varlıklı C (2015) Studies on UV-vis and fluorescence changes in Co^{2+} and Cu^{2+} recognition by a new benzimidazole-benzothiadiazole derivative. *Sensor Actuat B Chem* 209:853–863
- Harris JD, Liu J, Carter KR (2015) Synthesis of π -bridged dually-dopable conjugated polymers from benzimidazole and fluorene: separating sterics from electronics. *Macromolecules* 48:6970–6977
- Ku J, Song S, Park SH, Lee K, Suh H, Lansac Y, Jang YH (2015) Palladium-assisted reaction of 2,2-dialkylbenzimidazole and its implication on organic solar cell performances. *J Phys Chem C* 119:14063–14075
- Schmidt H (1997) Indigo—100 Jahre industrielle synthese. *Chem Unserer Zeit* 31:121–128

20. Kotha S, Lahiri K, Kashinath D (2002) Recent applications of the Suzuki-Miyaura cross-coupling reaction in organic synthesis. *Tetrahedron* 58:9633–9695
21. Saltan GM, Dinçalp H, Kıran M, Zafer C, Erbaş SÇ (2015) Novel organic dyes based on phenyl-substituted benzimidazole for dye sensitized solar cells. *Mater Chem Phys* 163:387–393
22. Icli S, İcil H (1996) A Thermal and photostable reference probe for Q_f measurements: chloroform soluble perylene 3,4,9,10-tetracarboxylic acid-bis-N,N-dodecyl diimide. *Spectrosc Lett* 29:1253–1257
23. Pommerehne J, Vestweber H, Guss W, Mahrt RF, Bassler H, Porsch M, Daub J (1995) Efficient 2-layer LEDs on a polymer blend basis. *Adv Mater* 7:551–554
24. Knutson JR, Beechem JM, Brand L (1983) Simultaneous analysis of multiple fluorescence decay curves - a global approach. *Chem Phys Lett* 102:501–507
25. Zuker M, Szabo AG, Bramall L, Krajcarski DT, Selinger B (1985) Delta-function convolution method (DFCM) for fluorescence decay experiments. *Rev Sci Instrum* 56:14–22
26. Frisch MJ, Trucks GW, Schlegel HB, Scuseria GE, Robb MA, Cheeseman JR, Scalmani G, Barone V, Mennucci B, Petersson GA, Nakatsuji H, Caricato M, Li X, Hratchian HP, Izmaylov AF, Bloino J, Zheng G, Sonnenberg JL, Hada M, Ehara M, Toyota K, Fukuda R, Hasegawa J, Ishida M, Nakajima T, Honda Y, Kitao O, Nakai H, Vreven T, Montgomery JA Jr, Peralta JE, Ogliaro F, Bearpark MJ, Heyd J, Brothers EN, Kudin KN, Staroverov VN, Kobayashi R, Normand J, Raghavachari K, Rendell AP, Burant JC, Iyengar SS, Tomasi J, Cossi M, Rega N, Millam NJ, Klene M, Knox JE, Cross JB, Bakken V, Adamo C, Jaramillo J, Gomperts R, Stratmann RE, Yazyev O, Austin AJ, Cammi R, Pomelli C, Ochterski JW, Martin RL, Morokuma K, Zakrzewski VG, Voth GA, Salvador P, Dannenberg JJ, Dapprich S, Daniels AD, Farkas Ö, Foresman JB, Ortiz JV, Cioslowski J, Fox DJ (2009) Gaussian 09. Gaussian, Inc., Wallingford
27. Kohn W, Sham LJ (1965) Self-consistent equations including exchange and correlation effects. *Phys Rev* 140:A1133–A1138
28. Goh C, Kline RJ, McGehee MD, Kadnikova EN, Frechet JMJ (2005) Molecular-weight-dependent mobilities in regioregular poly(3-hexyl-thiophene) diodes. *Appl Phys Lett* 86(1–3):122110
29. Carbone A, Kotowska BK, Kotowski D (2005) Space-charge-limited current fluctuations in organic semiconductors. *Phys Rev Lett* 95(1–4):236601
30. De Melo JS, Rondao R, Burrows HD, Melo MJ, Navaratnam S, Edge R, Voss G (2006) Spectral and photophysical studies of substituted indigo derivatives in their keto forms. *Chemphyschem* 7:2303–2311
31. Issa YM, Hassib HB, Abdelaal HE, Kenawi IM (2011) Spectral investigation of the intramolecular charge-transfer in some aminotriazole Schiff bases. *Spectrochim Acta A Mol Biomol Spectrosc* 79:1364–1374
32. Gan X, Liu G, Chu M, Xi W, Ren Z, Zhang X, Tian Y, Zhou H (2016) Intermolecular interactions boost aggregation induced emission in carbazole Schiff base derivatives. *Org Biomol Chem* 15:256–264
33. Kulhanek J, Bures F (2012) Imidazole as a parent pi-conjugated backbone in charge-transfer chromophores. *Beilstein J Org Chem* 8:25–49
34. Thanikachalam V, Arunpandian A, Jayabharathi J, Ramanathan P (2014) Photophysical properties of the intramolecular excited charge-transfer states of π -expanded styryl phenanthrimidazoles—effect of solvent polarity. *RSC Adv* 4:6790–6806
35. Pina J, Seixas De Melo JS, Eckert A, Scherf U (2015) Unusual photophysical properties of conjugated, alternating indigo-fluorene copolymers. *J Mater Chem A* 3:6373–6382
36. Rondao R, Seixas De Melo J, Schaberle FA, Voss G (2012) Excited state characterization of a polymeric indigo. *Phys Chem Chem Phys* 14:1778–1783